HHS Public Access

Author manuscript

Neuropharmacology. Author manuscript; available in PMC 2017 April 07.

Published in final edited form as:

Neuropharmacology. 2014 June ; 81: 274–282. doi:10.1016/j.neuropharm.2014.02.012.

Modulation of HCN channels in lateral septum by nicotine

Sodikdjon A. Kodirov[1,2,*], **Michael Wehrmeister**[1,3], and **Luis V. Colom**[1]

[1]Center for Biomedical Studies, Department of Biological Sciences, University of Texas at Brownsville, Texas 78520, USA

[2]Department of Molecular Physiology & Biophysics, University of Iowa, Iowa City, IA 52252, USA

[3]Johannes Gutenberg University, 55099 Mainz, Germany

Abstract

The effects of addictive drugs most commonly occur via interactions with target receptors. The same is true of nicotine and its multiple receptors in a variety of cell types. However, there are also side effects for given substances that can dramatically change cellular, tissue, organ, and organism functions.

In this study, we present evidence that nicotine possesses such properties, and modulates neuronal excitability. We recorded whole-cell voltages and currents in neurons situated in the dorsal portion of the lateral septum in acute coronal brain slices of adult rats. Our experiments in the lateral septum revealed that nicotine directly affects HCN – hyperpolarization-activated cyclic nucleotide gated non-selective cation channels.

We demonstrate that nicotine effects persist despite the concurrent application of nicotinic acetylcholine receptors' antagonists – mecamylamine, methyllycaconitine, and dihydro-β-erythroidine. These results are novel in regard to HCN channels in the septum, in general, and in their sensitivity to nicotine, in particular.

Keywords

Septal neurons; HCN channels; Action potentials; Sag potential; h-current

1. Introduction

The direct and indirect involvement of the septum in memory formation is a long-standing research interest. There are three major nuclei in this region: lateral septum (LS), medial septum (MS), and diagonal band of Broca (DBB). The LS is modulated by excitatory afferents from the hippocampus and is involved in synaptic plasticity. The hippocampus, in turn, receives the cholinergic and GABAergic inputs from MS and DBB. Thus, there is a

*Corresponding author. Department of Molecular Physiology & Biophysics, University of Iowa, 51 Newton Rd. 5-611 BSB, Iowa City, IA 52252, USA, Tel.: +1–319–3841763, Sodikdjon-Kodirov@uiowa.edu.

reciprocal interaction between the septum and the hippocampus (Vinogradova, 2001). The main function of the septum is to initiate and maintain the rhythmical slow wave activity (RSA), or the theta (θ) rhythm, in the hippocampus (Klemm, 1976). Memory formation requires a cross talk between the MS and the hippocampus via the generation and the subsequent modulation of θ–rhythm. The spikes in a majority of MS neurons exhibit a cross-correlation with the hippocampal θ–rhythm (Bland and Colom, 1993). However, only a subset of LS neurons oscillates in concert with the θ activity in the hippocampus (Pedemonte et al., 1998). Therefore, neurons of the MS can be considered pacemakers for the hippocampus.

The generation of a pacemaker signal – recurrent spontaneous slow depolarization – in two vital organs, the heart and brain, is caused by the presence and subsequent recurrent activation of hyperpolarization-activated cyclic nucleotide (HCN or I_h) gated non-selective cation channels (DiFrancesco et al., 1991; Solomon et al., 1993; Luthi and McCormick, 1998; Santoro and Tibbs, 1999; Inyushin et al., 2010). HCN channels and underlying currents carried many different nomenclatures (Brown et al., 1979), both in vertebrates and invertebrates (Noble and Tsien, 1968; Halliwell and Adams, 1982; Edman et al., 1987; Solomon et al., 1993; Araque et al., 1995), until they were established as I_f (funny) because of their uncommon gating properties (Altomare et al., 2001; Bucchi et al., 2002). Extensive study and discussion have occurred regarding the way HCN channels may modulate neuronal properties (their inputs and outputs) and to what extent the alpha subunit along the auxiliary TRIP8b (tetratricopeptide containing Rab8b-interacting protein) subunit tune synaptic plasticity and depressive behavior in rodents (Brager et al., 2013; Lewis et al., 2011).

The functions of the MS and properties of its neurons have also been extensively studied (Thinschmidt et al., 2005; Butuzova and Kitchigina, 2008); however, there are scant investigations on the LS in this regard. The purpose of this study is to elucidate the additional target(s) of nicotine at the cellular level in the septum and to advance our understanding of underlying mechanisms of addiction. Our results demonstrate, for the first time, that HCN channels are present in a subpopulation of LS neurons. Further experiments reveal modulation of these channels by nicotine and facilitated excitability in the majority of cells studied. We also consider novel direct effects of nicotine on HCN channels, since this study was designed and planned independently (Wehrmeister et al., 2010) of another recently published article (Griguoli et al., 2010).

2. Materials and methods

All experiments were conducted at room temperature (22–24°C).

2.1. Slice preparation

Conditions and procedures for the preparation of coronal brain slices (300 μm) containing septum (Fig. 1) were similar to those previously described (Kodirov et al., 2010). Sprague Dawley rats (P34.5 ± 1.4, $n = 33$) were anaesthetized with isoflurane before the preparation. Animal use was in accordance with the NIH guide for the care and use of laboratory animals, and all procedures were approved by the local committee.

2.2. Electrophysiology

Whole-cell voltage– and current–clamp recordings were obtained from heterogeneous subpopulations of neurons in the dorsal part of the lateral nuclei of the septum using the patch–clamp technique (Hamill et al., 1981). Slices were allowed to recover from preparation procedures for at least 1 hour. Electrode resistance ranged between 2 and 6 MΩ when filled with an intracellular solution. Series resistance was monitored during the course of each experiment. It consistently did not exceed 30 MΩ and was not compensated. The input resistance (IR) of cells had a mean value of 233.1 ± 10.4 MΩ (n = 50). Action potentials (APs) and sag were evoked in response to a depolarizing and hyperpolarizing current injections (up to ±300 pA), respectively. Types of cells were identified by either the presence or the absence of I_h-mediated sag in membrane potential/current (Fig. 2A and B). The sag is the portion of membrane potential (MP) that spontaneously depolarizes compared to the peak during negative pulses. The sag amplitude (Fig. 2A) was estimated by subtracting values at the onset of hyperpolarizing currents/voltages (peak amplitude) from those at the end (steady-state). The I_h current was recorded in the presence of 1 mM 4–aminopyridine (4–AP), 1 mM Co^{2+}, 1 μM tetrodotoxin (TTX), or 100–300 μM Ba^{2+} in order to isolate it from possible contamination by voltage dependent K^+, L–type Ca^{2+}, Na^+ and inward rectifier K^+ channels, respectively (Griffith, 1988; Kodirov et al., 2003; Kodirov et al., 2004). The current signals were filtered at 1 kHz and the sampling interval was 2.5–5 kHz. The analyses and subtraction of traces were performed using Clampfit software (Axon Instruments).

2.3. Solutions

The artificial cerebrospinal fluid (ACSF) contained (in mM) 119 NaCl, 2.5 KCl, 1.25 NaH_2PO_4, 1 $MgSO_4$, 2.5 $CaCl_2$, 26 $NaHCO_3$, and 10 glucose. This solution was equilibrated with 95% O_2 and 5% CO_2 (pH = 7.4) and was also used for the brain slice preparation. The pipette solution was composed (in mM) of 120 K^+–gluconate, 5 NaCl, 1 $MgCl_2$, 10 HEPES, 0.2 EGTA, 2 Mg_2ATP, and 0.2 NaGTP (pH = 7.2). Nicotine was purchased in liquid form and diluted in equilibrated ACSF to achieve final concentrations as indicated in **Results**. Stock solutions of ZD 7288, mecamylamine (MEC), methyllycaconitine (MLA), 4-AP, TTX, Ba^{2+}, and Co^{2+} were prepared using distilled water; dihydro-β-erythroidine (DHβE) was dissolved in ethanol.

2.4. Statistical tests

The data are presented as the mean ± SE, where n corresponds to the number of experiments. The effects of substances were tested in the same neuron after obtaining the baseline response under control conditions. Each slice was used only for one experimental set involving pharmacology, i.e. they were not reused after the wash-out. Student's t test was used for data group comparison; $P < 0.05$ was considered significant.

3. Results

We have characterized the properties of membrane and action potentials of neurons strictly in the dorsal part of the lateral septum (LS) as indicated in Figure 1.

3.1. Presence of HCN channels

The LS neurons consist of two groups that were distinguished by the absence (Fig. 2B) or the presence of depolarizing sag (Fig. 2A), which is mediated by I_h activation upon hyperpolarization. The mean values of resting membrane potentials (RMP) in neurons exhibiting I_h-mediated depolarizing sag was −59.5 ± 1.3 mV (n = 9). The neurons, which did not show a typical and prominent sag, had a mean RMP of −58.2 ± 2 mV (n = 9, P = 0.6); thus, differences are not related to RMP values. Note that if sag was present in a recorded cell, it was already measurable upon application of currents of moderate magnitude (−120 pA; Fig. 2A). However, in some neurons, even strong pulses (−300 pA) did not lead to the activation of I_h channels that are evidenced by the absence of depolarizing sag. Thus, among recorded neurons, two groups in regard to either the presence or the absence of sag could be clearly defined (indicated by blue and red lines, respectively; Fig. 2C). The average value of sag amplitudes under baseline conditions in LS cells was −12.1 ± 2.1 mV (at −300 pA, n = 9,●; Fig. 2D). Note that in two out of these 9 cells, the highest amplitude was observed. In the remaining neurons, no significant sag was observed in response to current steps ranging between −20 and −300 pA (−1.1 ± 0.4 mV, n = 8, ●; Fig. 2D). The relationship between the sag amplitude and the applied current magnitude in the two groups was either exponential (red line) or linear (blue, Fig. 2D).

3.2. Modulation of excitability by nicotine

The facilitated excitability of neurons was manifested by their vulnerability to trigger an increased number of APs in the presence of nicotine. The APs were always evoked from the RMP by the injection of constant depolarizing currents of up to 300 pA in magnitude and 1 s in duration. Properties of the membrane and APs were analyzed in the same neurons under control conditions (Fig. 3A), in the presence of 3 μM nicotine (Fig. 3B), and upon wash-out (Fig. 3C). The APs were elicited upon application of 40 pA steps, and employing −300 pA enabled the sag in membrane potential (MP) at the beginning of the current step, which declined in amplitude within 1 s. In some cells, rebound action potentials (RAP) were triggered upon termination of hyperpolarizing pulses ranging from −300 to −100 pA (Fig. 3A). There is a correlation between the sag (presence of I_h) and RAP, since both are eliminated by ZD 7288 (Lewis et al., 2011). Application of 3 μM nicotine increased the frequency of APs elicited by both the depolarization and preceding hyperpolarization (Fig. 3B).

Other remarkable changes that we have observed in the presence of nicotine are “double spikes” in which the second AP is triggered during the incomplete repolarization phase of the first AP. Two spikes in close proximity occurred only at the beginning of each depolarizing step, whereas subsequent APs exhibited regular intervals. The same phenomenon was also observed during the RAPs (Fig. 3H), and the second AP was tightly coupled with the first AP only at the beginning of each train of APs evoked upon the termination of hyperpolarizing 1 s steps. Under control conditions (Fig. 3G), both AP and RAP were only followed by ADP (after depolarizing potentials), not by the second low amplitude spike.

The effects of nicotine were, to a significant extent, reversible, depending on certain parameters (Fig. 3D–F). Thus, the amplitudes of APs were significantly decreased after nicotine wash-in (Fig. 3B and E), which was reversed during the ~30 min wash-out. Interestingly, the frequency of APs increased further (Fig. 3C). The peak amplitude of MP was also reversibly increased by nicotine (Fig. 3D). An increase in the excitability of neurons can also be concluded based on the fact that, during wash-in and wash-out of nicotine, a much lower current injection was necessary in order to trigger APs: 40 vs. 20 pA in the absence and the presence of nicotine, respectively (Fig. 3E). In the majority of cells (8 out of 12) nicotine increased the frequency of APs.

In the remaining cells, nicotine significantly decreased the frequency of APs (Fig. 4A–C). Similar tendencies were observed in laterodorsal tegmental neurons (Ishibashi et al., 2009). In Figure 4, the responses to depolarizing (180 pA, red traces) and hyperpolarizing (−280 pA, black) current steps are superimposed. The effects of nicotine were independent from the basal frequency of APs. The frequency diapason in corresponding groups before the application of nicotine was similar (1–11 vs. 1–10 Hz). Therefore, the average values were also not significantly different ($P = 0.6$, unpaired t test). Next, a decrease in AP numbers exacerbated by nicotine was accompanied by an increase in amplitude (Fig. 4B), which can be judged by overshoot potentials (the range above upper dashed lines at identical ±0 mV levels). This was opposite in the first group, i.e. an increase in frequency correlated with a decrease in amplitude (Fig. 3B and E).

The presence of I_h (–mediated sag) and its subsequent significant activation by hyperpolarizing currents was often followed by rebound tail potential (RTP). Depending on the magnitude of sag, the RTP can reach a threshold for the generation of RAP as shown in Figure 3A and G. We have analyzed experiments in which the sag resulted in RTP, yet no RAP was observed (Fig. 4D). The mean amplitude of sag potential (−5.7 ± 0.8 mV at −280 pA) was approximately two-fold greater than that of RTP (2.9 ± 0.8 mV, $n = 6$, $P = 0.002$; Fig. 4E). Further analyses revealed a linear relationship between the amplitude(s) of sag and RTP ($R = 0.99$; Fig. 4F).

3.3. Nicotine-mediated sag

Nicotine application not only significantly increased the amplitude of sag, but it also led to the appearance of voltage sag, albeit with slower kinetics (Fig. 5B), even in cells that did not initially exhibit such a response (Fig. 5A). Nicotine increased the peak amplitudes (Fig. 5C) in 10 out of 12 cells. Note that dual effects of nicotine have also been observed for GABAergic synaptic inputs in some dopaminergic (DA) neurons in the ventral tegmental area (VTA) of mesencephalon and their APs (Mansvelder et al., 2002). In Figure 5D, the normalized (% of baseline; ●) values of steady–state amplitude, at −300 pA, under control conditions and in the presence of nicotine (●), are shown for individual cells. The mean value increased from −48.8 ± 2.2 to −63.4 ± 3.6 mV ($n = 10$, $P = 0.001$, Fig. 5E). The RMP remained unaffected in the presence of nicotine (−58.5 ± 1.7 vs. −59.5 ± 2.1 mV; $n = 10$, $P = 0.5$). Nicotine did not affect the amplitude of MP upon depolarization (44.9 ± 3.1 *vs.* 47.4 ± 2.9 mV at 300 pA, $n = 10$, $P = 0.2$; Fig. 5E). Our conclusion is two-fold in this regard: 1) consistently, I_h activates only upon hyperpolarization and does not significantly contribute to

the steady–state MP at depolarized potentials; 2) nicotine to some extent affects the I_h selectively, since the peak MP increased and its waveform resembled the sag potential (Fig. 5).

3.4. Nicotine effects do not involve nAChRs

We have performed further experiments by directly inhibiting the nicotinic acetylcholine receptors (nAChRs). Multiple distinct subunits of nAChRs are located within several brain areas. Among all nAChRs, those composed of α7 or containing β2 subunits (β2*) are most predominant in the brain. Therefore, we focused on these subunits and their selective antagonists during the experiments with neurons of the LS. Similar to previous experiments, we have applied an identical concentration of nicotine in the presence of DHβE (0.1–1 μM), the selective antagonist of β2 subunits containing nAChRs. However, this approach did not result in a conclusive outcome. The dual nicotine effects were similar in the presence of both 100 nM (Fig. 6B) and 1 μM DHβE (Fig. 6D). All nine cells tested were susceptible to nicotine, and, in six out of nine neurons (○), an increase in HCN channel-mediated sag (Fig. 6A and D) and resultant RTP was observed; in three cells (○), nicotine decreased these parameters. The mean values (Fig. 6B) in these two groups were −74.0 ± 8.7 mV (n = 6) and −34.2 ± 5.8 mV (n = 3), respectively, while control values (●) were −55.4 ± 6.2 mV (n = 9). Therefore, the outcomes of the pooled data (○) shown in Figure 6C (n = 9) cannot be taken into account. At this point, we have concluded that nicotine does not recruit the β2* nAChRs' dependent pathways. Since, theoretically, LS neurons may express only one or both subunits, we tested for either the presence or the absence of α7-containing nAChRs, which are sensitive to methyllycaconitine (MLA). Further experiments were performed in a similar manner, but instead of DHβE, we used 0.1–1 μM MLA (Fig. 6E, n = 7), which did not influence nicotine's effects. Next, we applied nicotine under the simultaneous inhibition of both receptor types using MLA and DHβE (Fig. 6F, n = 7). Despite these modifications, the overall tendencies with nicotine effects were similar to those initially presented.

3.5. Support for HCN channel expression in the LS

We have performed additional analyses by recording currents instead of potentials. However, each experiment was initiated similar to previous ones by recording the MP and APs. Consistently, typical sag was observed during hyperpolarization (Fig. 7A). Next, in the same neurons, the I_h was activated using the protocol shown in Figure 7D. Consistently, the presence of sag in MP correlated well with slowly activating currents (red arrow) upon hyperpolarization ranging between −140 and −100 mV (Fig. 7B and F). Application of selective antagonist of HCN channels, ZD 7288, at 1 and 10 μM concentrations significantly decreased the amplitude (Fig. 7C and D, respectively). Note that tail currents (Lyashchenko and Tibbs, 2008), activated upon the termination of hyperpolarization, are also inhibited by this blocker in a dose dependent manner (blue arrow). I_h was observed readily upon strong hyperpolarization, and, at −90 mV, their equilibration times were slow, as previously observed (Mannikko et al., 2005). By estimating the difference in the amplitude of currents immediately upon hyperpolarization and at the end of a 4 s pulse, the magnitude of sag was revealed for each cell. Consistently, also in regard to I_h, two groups were distinguished (Fig. 7F). In the majority of LS cells (8 out of 12), a clear sag in membrane currents was observed (●), and in the remaining four neurons, HCN channels were absent (○). The steady-state I_h

was inhibited by 1 μM ZD 7288 (Fig. 7E), and at 10 μM concentration the remaining currents activated instantaneously (Rivera-Arconada et al., 2013). The overall responses to hyperpolarizing potentials were similar to those described in olfactory neurons (Vargas and Lucero, 2002). Note that our experimental conditions were different, particularly in regard to the holding potential, which is often set to around −50 mV (Tabarean et al., 2012).

3.6. Direct modulation of I_h by nicotine

Due to activation of additional channels by hyperpolarization, the presence of depolarizing sag in MP is not always considered to be solely attributed to the activation of HCN channels. For this reason, we have recorded I_h in isolation.

Prior to the application of nicotine (Fig. 8B), stable recordings revealing the presence of I_h in neurons were obtained at a holding potential of −70 mV (Fig. 8A). The current waveforms in different LS neurons were closely reproducible, and application of 3 μM nicotine for 15 min resulted in a dual response. Nicotine either increased ($n = 5$) or decreased I_h ($n = 6$) when tested at −130 mV (Fig. 8D). The activation kinetics of I_h in the absence and presence of nicotine were similar (Fig. 8C, traces are recorded at −140 mV). The subtracted nicotine-sensitive currents (Fig. 8E) were relatively small. They are represented using identical time and amplitude scales, as for Figure 8A and B, in order to define a possible change in IR, which was minimal in this case.

Finally, under voltage clamp conditions, we have tested mecamylamine (MEC), another nonselective inhibitor of nAChRs, at concentrations ranging between 100 nM and 10 μM (Fig. 8F). The dual nicotine effects also remained unaltered after a long perfusion with a high concentration of MEC (10 μM), and nicotine either increased (by 138.2 ± 14.9 %, n = 4) or decreased (81.1 ± 19.7 %, $n = 2$; at −120 pA) I_h. Therefore, evidently, nicotine directly modulates I_h and the resultant sag. The latter is in agreement with recent study showing direct binding of nicotine along its analog epibatidine to HCN channels (Griguoli et al., 2010).

3.7. Nicotine dose response

At 300 nM concentration, nicotine was less effective; however, a similar tendency (see Fig. 5) was observed in the response of neurons: sag either increases ($n = 2$), decreases ($n = 1$) or remains unchanged ($n = 4$). Note that the effects varied cell to cell. Since, at this concentration, two groups were not clearly distinguishable, we did not pursue further experiments. However, we have performed additional experiments with two cumulative doses of nicotine in order to avoid the overall neuron to neuron variations in certain parameters and time dependent changes in patch quality. During these experiments, we have decreased the time of exposure as well, but kept both conditions similar (~6 min). The inhibition by 31 % at 1 μM is comparable to results of Griguoli et al. (2010). The effects are saturated around this level despite the increased concentration of nicotine. Note that, in the text, the latter authors refer to 10 μM, but it is actually at 1 μM nicotine concentration that the magnitude of inhibition was 39 %, which decreased at 10 μM to ~32 %. Thus, our data, similar to those of Griguoli et al. (2010), reveal a fast saturation in dose responses. We did

not test additional higher concentrations, since they would be irrelevant to human studies (see Discussion).

4. Discussion

Nicotine possesses multiple targets in regard to brain areas, ion channels, and receptors, and thus is involved in several pathologies (Dani and Bertrand, 2007).

In this study, we demonstrate the dual effects (prevailing excitation *vs.* inhibition) of nicotine on a distinct population of neurons in the septum. The extracellular application of nicotine increased the frequency of APs elicited by both depolarization and preceding hyperpolarization (Fig. 3B) and, in some neurons, triggered “double spikes” (Fig. 3H). The nicotine application led to the appearance of voltage sag in cells which did not initially significantly exhibit such a response upon hyperpolarization (Fig. 5). The voltage sag under these conditions had slower kinetics. We suggest that it might be related to expression of distinct subunits in different cell types (Leao et al., 2006; George et al., 2009).

Our concentration choice was relied on available data on smokers, in particular on one study by Henningfield and colleagues (1993). They have documented that the level of arterial nicotine was, on average, around 1.18 μM, and the latter was dependent on individuals tested. Also in the literature, one can find an even higher concentration of nicotine used during physiological experiments depending on application methods, e.g. either incubation or a puff. Dual effects, i.e. facilitation or inhibition, were also observed during cumulative nicotine application to LS neurons. Under identical experimental conditions, facilitation saturated at 3 μM nicotine concentration, while inhibition was already saturated at 1 μM. The EC_{50} for facilitation was 0.92 μM, which is close to the data of Henningfield et al. (1993), but higher than the documented 62 nM in CA1 interneurons (Griguoli et al., 2010).

The major effects – facilitated excitability – occurred via modulation of I_h and underlying sag. Our data reveal that α7 and β2 nAChRs do not contribute to nicotine and I_h interactions (Fig. 6 and Fig. 8). In our experiments, nicotine effects were not completely reversible during up to 30 min of wash-out. Reversible effects of nicotine, to greater extent, have been observed on APs of DA neurons of VTA (Mansvelder et al., 2002). These dissimilarities might be related to differences in nicotine exposure time.

The sag was mediated by I_h, and based on equilibration time, we suggest that the underlying channels could be either HCN1 or HCN2, but not HCN4 (Altomare et al., 2001). These currents were inhibited by 1 μM ZD 7288 (Fig. 7). At a higher concentration, also, tail currents were completely blocked. The blockade of I_h by ZD 7288 and the subsequent effects on the passive properties of MP often are not consistent, since it either increases (George et al., 2009) or decreases the IR (Sotty et al., 2003). In the MS/DBB neurons, 10 μM ZD 7288 appeared to selectively block the sag. However, in this case, a significant increase in IR was observed (Morris et al., 2004). Similar to above-mentioned studies, ZD 7288 increased the IR of LS neurons by 50–100 MΩ. Interestingly, this compound eliminates rebound APs only in certain types of neurons (Leao et al., 2006), but not in MS/DBB despite an increase in their latencies (Morris et al., 2004).

Similar to other ion channels, the electrophysiological properties of I_h are complete when an adequate auxiliary subunit(s) interact with the alpha subunit. The absence of TRIP8b eliminates the HCN-mediated phenotype, i.e. the sag and RTP in CA1 pyramidal neurons (Brager et al., 2013). The sag and RTP in wild type mice are blocked by 20 μM ZD 7288. These effects are accompanied by an increase in the IR, while in TRIP8b KO it slightly decreased the IR (Lewis et al., 2011).

5. Conclusions

In conclusion, our results demonstrating I_h in LS are novel particularly in their modulation by nicotine. This channel and its subsequent modulation by relatively low concentration of nicotine (Goriounova and Mansvelder, 2012) may play a functional role in the synergistic synaptic plasticity and development of related memories in the septo–hippocampal complex. Moreover, because of the established involvement of HCN in epilepsy (Budde et al., 2005), nicotine could be used to target these channels at the neuronal level. The direct effects of nicotine are potentially important for addiction, since the duration of action on HCN channels is prolonged when compared to nAChRs fast desensitization.

Acknowledgements

All authors appreciate the animal care and rats provided by Jennifer Bagley. S.A.K. greatly appreciates Marcos Cantu and Samantha Rendon in their eagerness to learn and participation during the conception of some experiments at earlier stages. We thank Boris Ermolinsky for multiple discussions in regard to the presented results, Michael Lehker and Melinda Smits for the reading of the manuscript, Nicholas D. Leymaster for invaluable inputs, Clara Downey-Adams and Catherine Miller for proof reading. This research was supported by the National Institute of Health. Finally, we would like to acknowledge two anonymous reviewers.

Abbreviations

AP	action potential
LS	lateral septum
HCN	hyperpolarization-activated cyclic nucleotide gated non-selective cation channel
RAP	rebound action potential
RTP	rebound tail potential
nAChRs	nicotinic acetylcholine receptors.

References

Altomare C, Bucchi A, Camatini E, Baruscotti M, Viscomi C, Moroni A, DiFrancesco D. Integrated allosteric model of voltage gating of HCN channels. J Gen Physiol. 2001; 117:519–532. [PubMed: 11382803]

Araque A, Cattaert D, Buno W. Cd^{2+} regulation of the hyperpolarization-activated current I_{AB} in crayfish muscle. J Gen Physiol. 1995; 105:725–744. [PubMed: 7561741]

Bland BH, Colom LV. Extrinsic and intrinsic properties underlying oscillation and synchrony in limbic cortex. Prog Neurobiol. 1993; 41:157–208. [PubMed: 8332751]

Brager DH, Lewis AS, Chetkovich DM, Johnston D. Short- and long-term plasticity in CA1 neurons from mice lacking h-channel auxiliary subunit TRIP8b. J Neurophysiol. 2013; 110:2350–2357. [PubMed: 23966674]

Brown H, Difrancesco D, Noble S. Cardiac pacemaker oscillation and its modulation by autonomic transmitters. J Exp Biol. 1979; 81:175–204. [PubMed: 315983]

Bucchi A, Baruscotti M, DiFrancesco D. Current-dependent block of rabbit sino-atrial node I_f channels by ivabradine. J Gen Physiol. 2002; 120:1–13. [PubMed: 12084770]

Budde T, Caputi L, Kanyshkova T, Staak R, Abrahamczik C, Munsch T, Pape HC. Impaired regulation of thalamic pacemaker channels through an imbalance of subunit expression in absence epilepsy. J Neurosci. 2005; 25:9871–9882. [PubMed: 16251434]

Butuzova MV, Kitchigina VF. Repeated blockade of $GABA_A$ receptors in the medial septal region induces epileptiform activity in the hippocampus. Neurosci Lett. 2008; 434:133–138. [PubMed: 18304731]

Dani JA, Bertrand D. Nicotinic acetylcholine receptors and nicotinic cholinergic mechanisms of the central nervous system. Annu. Rev. Pharmacol. Toxicol. 2007; 47:699–729. [PubMed: 17009926]

DiFrancesco D, Porciatti F, Janigro D, Maccaferri G, Mangoni M, Tritella T, Chang F, Cohen IS. Block of the cardiac pacemaker current (If) in the rabbit sino-atrial node and in canine Purkinje fibres by 9-amino-1,2,3,4- tetrahydroacridine. Pflugers Arch. 1991; 417:611–615. [PubMed: 2057325]

Edman A, Gestrelius S, Grampp W. Current activation by membrane hyperpolarization in the slowly adapting lobster stretch receptor neurone. J Physiol. 1987; 384:671–690. [PubMed: 2443664]

George MS, Abbott LF, Siegelbaum SA. HCN hyperpolarization-activated cation channels inhibit EPSPs by interactions with M-type K^+ channels. Nat Neurosci. 2009; 12:577–584. [PubMed: 19363490]

Goriounova NA, Mansvelder HD. Nicotine exposure during adolescence leads to short- and long-term changes in spike timing-dependent plasticity in rat prefrontal cortex. J Neurosci. 2012; 32:10484–10493. [PubMed: 22855798]

Griffith WH. Membrane properties of cell types within guinea pig basal forebrain nuclei in vitro. J Neurophysiol. 1988; 59:1590–1612. [PubMed: 3385475]

Griguoli M, Maul A, Nguyen C, Giorgetti A, Carloni P, Cherubini E. Nicotine blocks the hyperpolarization-activated current I_h and severely impairs the oscillatory behavior of oriens-lacunosum moleculare interneurons. J Neurosci. 2010; 30:10773–10783. [PubMed: 20702707]

Halliwell JV, Adams PR. Voltage-clamp analysis of muscarinic excitation in hippocampal neurons. Brain Res. 1982; 250:71–92. [PubMed: 6128061]

Hamill OP, Marty A, Neher E, Sakmann B, Sigworth FJ. Improved patch-clamp techniques for high-resolution current recording from cells and cell-free membrane patches. Pflugers Arch. 1981; 391:85–100. [PubMed: 6270629]

Henningfield JE, Stapleton JM, Benowitz NL, Grayson RF, London ED. Higher levels of nicotine in arterial than in venous blood after cigarette smoking. Drug Alcohol Depend. 1993; 33:23–29. [PubMed: 8370337]

Inyushin MU, Arencibia-Albite F, Vázquez-Torres R, Vélez-Hernández ME, Jiménez-Rivera CA. Alpha-2 noradrenergic receptor activation inhibits the hyperpolarization-activated cation current (I_h) in neurons of the ventral tegmental area. Neuroscience. 2010; 167:287–297. [PubMed: 20122999]

Ishibashi M, Leonard CS, Kohlmeier KA. Nicotinic activation of laterodorsal tegmental neurons: implications for addiction to nicotine. Neuropsychopharmacology. 2009; 34:2529–2547. [PubMed: 19625996]

Klemm WR. Physiological and behavioral significance of hippocampal rhythmic, slow activity ("theta rhythm"). Prog Neurobiol. 1976; 6:23–47. [PubMed: 778917]

Kodirov SA, Brunner M, Busconi L, Koren G. Long-term restitution of 4-aminopyridine-sensitive currents in Kv1DN ventricular myocytes using adeno-associated virus-mediated delivery of Kv1.5. FEBS Letters. 2003; 550:74–78. [PubMed: 12935889]

Kodirov SA, Jasiewicz J, Amirmahani P, Psyrakis D, Bonni K, Wehrmeister M, Lutz B. Endogenous cannabinoids trigger the depolarization-induced suppression of excitation in the lateral amygdala. Learn Mem. 2010; 17:43–49. [PubMed: 20042481]

Kodirov SA, Zhuravlev VL, Pavlenko VK, Safonova TA, Brachmann J. K^+ channels in cardiomyocytes of the pulmonate snail Helix. J. Membr. Biol. 2004; 197:145–154. [PubMed: 15042346]

Leao KE, Leao RN, Sun H, Fyffe RE, Walmsley B. Hyperpolarization-activated currents are differentially expressed in mice brainstem auditory nuclei. J Physiol. 2006; 576:849–864. [PubMed: 16916913]

Lewis AS, Vaidya SP, Blaiss CA, Liu Z, Stoub TR, Brager DH, Chen X, Bender RA, Estep CM, Popov AB, Kang CE, Van Veldhoven PP, Bayliss DA, Nicholson DA, Powell CM, Johnston D, Chetkovich DM. Deletion of the hyperpolarization-activated cyclic nucleotide-gated channel auxiliary subunit TRIP8b impairs hippocampal I_h localization and function and promotes antidepressant behavior in mice. J Neurosci. 2011; 31:7424–7440. [PubMed: 21593326]

Luthi A, McCormick DA. H-current: properties of a neuronal and network pacemaker. Neuron. 1998; 21:9–12. [PubMed: 9697847]

Lyashchenko AK, Tibbs GR. Ion binding in the open HCN pacemaker channel pore: fast mechanisms to shape "slow" channels. J Gen Physiol. 2008; 131:227–243. [PubMed: 18270171]

Mannikko R, Pandey S, Larsson HP, Elinder F. Hysteresis in the voltage dependence of HCN channels: conversion between two modes affects pacemaker properties. J Gen Physiol. 2005; 125:305–326. [PubMed: 15710913]

Mansvelder HD, Keath JR, McGehee DS. Synaptic mechanisms underlie nicotine-induced excitability of brain reward areas. Neuron. 2002; 33:905–919. [PubMed: 11906697]

Mikula S, Trotts I, Stone JM, Jones EG. Internet-enabled high-resolution brain mapping and virtual microscopy. NeuroImage. 2007; 35:9–15. [PubMed: 17229579]

Morris NP, Fyffe RE, Robertson B. Characterisation of hyperpolarization-activated currents (I_h) in the medial septum/diagonal band complex in the mouse. Brain Res. 2004; 1006:74–86. [PubMed: 15047026]

Moore AR. The selective action of nicotine on the central nervous system of the squid, *Loligo Pealii*. J Gen Physiol. 1919; 1:505–508. [PubMed: 19871764]

Noble D, Tsien RW. The kinetics and rectifier properties of the slow potassium current in cardiac Purkinje fibres. J Physiol. 1968; 195:185–214. [PubMed: 5639799]

Pedemonte M, Barrenechea C, Nunez A, Gambini JP, Garcia-Austt E. Membrane and circuit properties of lateral septum neurons: relationships with hippocampal rhythms. Brain Res. 1998; 800:145–153. [PubMed: 9685619]

Rivera-Arconada I, Roza C, Lopez-Garcia JA. Characterization of hyperpolarization-activated currents in deep dorsal horn neurons of neonate mouse spinal cord in vitro. Neuropharmacology. 2013; 70:148–155. [PubMed: 23376246]

Santoro B, Tibbs GR. The HCN gene family: molecular basis of the hyperpolarization-activated pacemaker channels. Ann N Y Acad Sci. 1999; 868:741–764. [PubMed: 10414361]

Solomon JS, Doyle JF, Burkhalter A, Nerbonne JM. Differential expression of hyperpolarization-activated currents reveals distinct classes of visual cortical projection neurons. J. Neurosci. 1993; 13:5082–5091. [PubMed: 8254362]

Sotty F, Danik M, Manseau F, Laplante F, Quirion R, Williams S. Distinct electrophysiological properties of glutamatergic, cholinergic and GABAergic rat septohippocampal neurons: novel implications for hippocampal rhythmicity. J Physiol. 2003; 551:927–943. [PubMed: 12865506]

Tabarean IV, Sanchez-Alavez M, Sethi J. Mechanism of H_2 histamine receptor dependent modulation of body temperature and neuronal activity in the medial preoptic nucleus. Neuropharmacology. 2012; 63:171–180. [PubMed: 22366077]

Thinschmidt JS, Frazier CJ, King MA, Meyer EM, Papke RL. Medial septal/diagonal band cells express multiple functional nicotinic receptor subtypes that are correlated with firing frequency. Neurosci Lett. 2005; 389:163–168. [PubMed: 16112453]

Vargas G, Lucero MT. Modulation by PKA of the hyperpolarization-activated current (I_h) in cultured rat olfactory receptor neurons. J Membr Biol. 2002; 188:115–125. [PubMed: 12172637]

Vinogradova OS. Hippocampus as comparator: role of the two input and two output systems of the hippocampus in selection and registration of information. Hippocampus. 2001; 11:578–598. [PubMed: 11732710]

Wehrmeister, M., Colom, LV., Kodirov, SA. Nicotine affects both the neuronal action and membrane potential's waveforms. 40th annual meeting of the Society for Neuroscience; San Diego, USA. 2010.

Highlights

- The manuscript is the first to demonstrate I_h channel in a subgroup of lateral septum (LS) neurons
- Nicotine directly affects I_h channels in LS neurons
- Nicotine effects is independent of nAChR activation

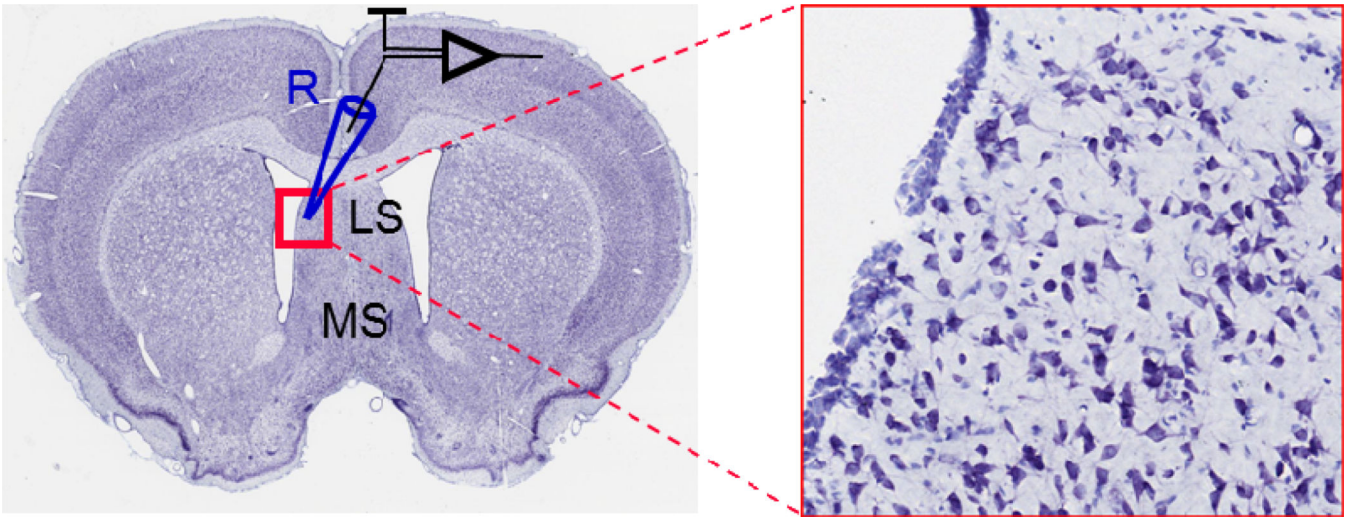

Fig. 1.

Coronal slice from rat brain and location of recorded neurons at higher magnification. R – recording electrode, LS – lateral septum, MS – medial septum. Modified from www.brainmaps.org (Mikula *et al.*, 2007).

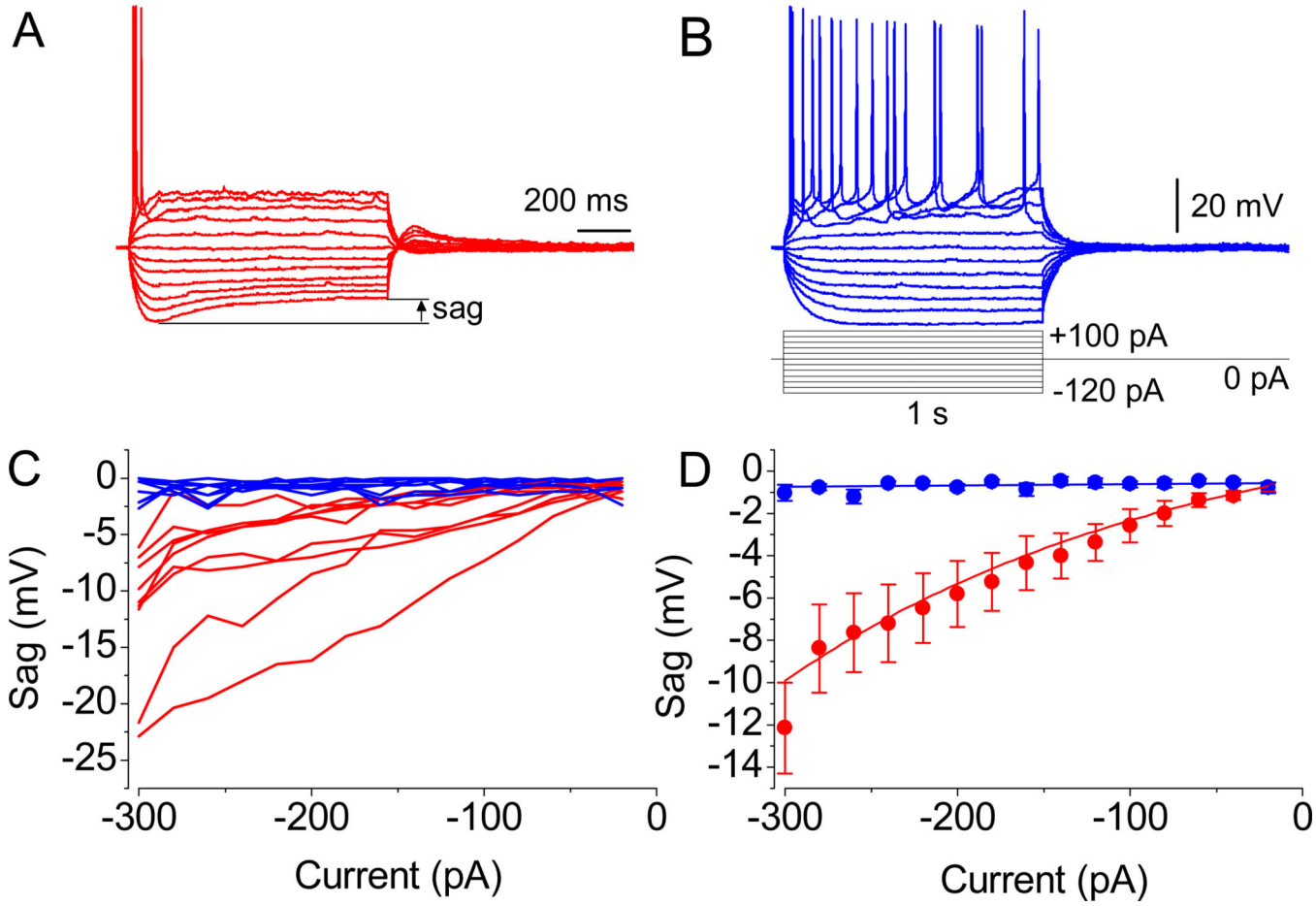

Fig. 2.

Action potential waveforms. (A and B) Evoked APs in two different neurons. Note the significant sag in MP in A and its absence in B, as revealed upon the injection of currents of relatively low amplitude. (C) Representation of sag's magnitude from all recorded neurons. (D) The mean amplitude values in cells with properties resembling the one shown in A (n = 9, $P < 0.01$ at −300 to −40 pA, paired t test) and B (n = 9, $P = 0.5$). Resting membrane potential was −55.2 mV in A and −52.2 mV in B. Identical scale bars are shown.

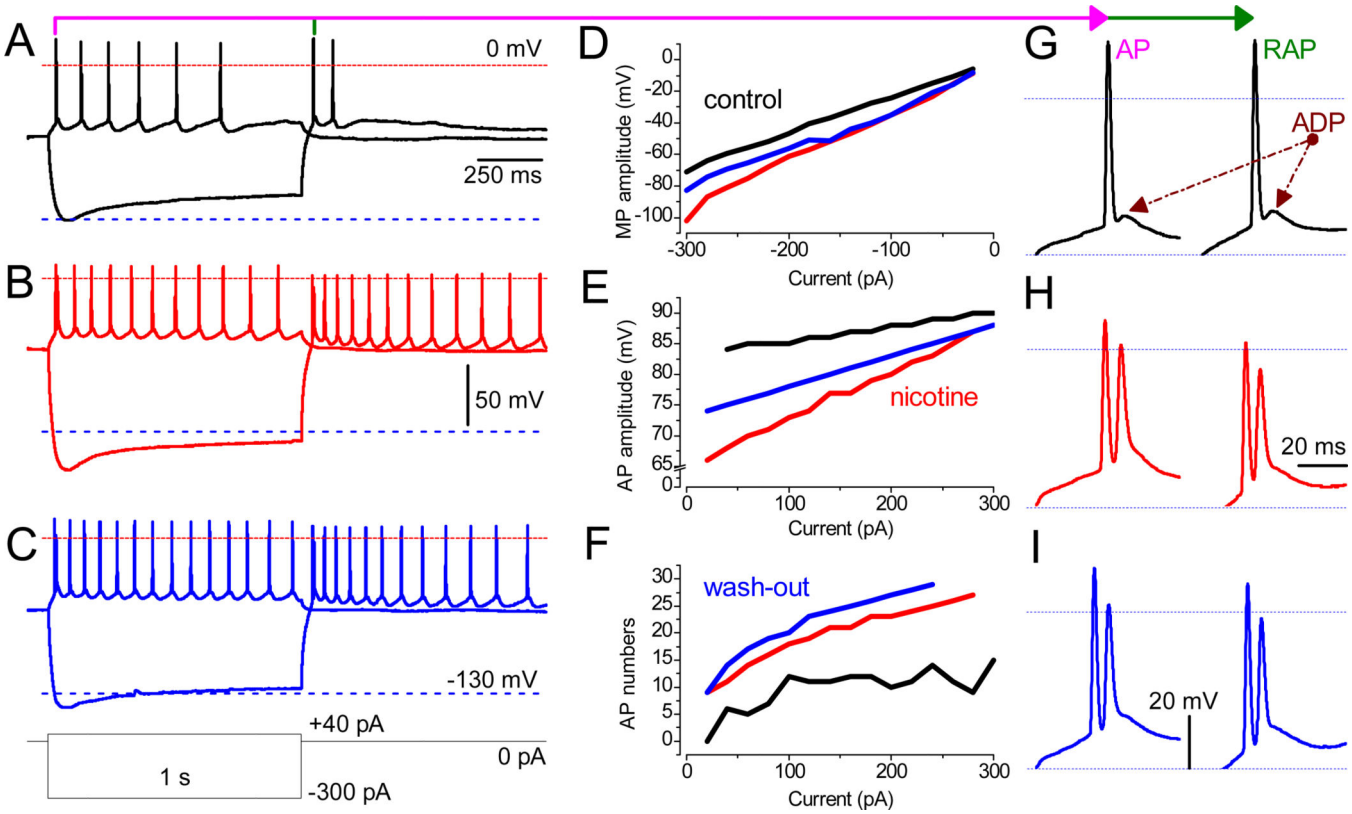

Fig. 3.

Nicotine facilitates neuronal excitably in LS. (A–C) Recordings were obtained from the same neuron in the absence and the presence of 3 μM nicotine and upon wash-out. The waveforms of MP during depolarizing (40 pA) and hyperpolarizing (−300 pA) current steps are superimposed. The red and blue dashed lines mark MP at ±0 mV and −130 mV, respectively. (D–F) Values before (black traces) and after the application of 3 μM nicotine (red) and upon the wash-out (blue). The analyzed parameters are: (D) the peak MP response to hyperpolarizing currents ranging from −20 pA to −300 pA in 20-pA increments; (E) the amplitude of the first AP upon depolarization by current steps (20–300 pA); (F) the number of APs per second. Note that, under control conditions, no AP was triggered at 20 pA (black). (G–I) The phenotype of both AP (left) and RAP (right) in a train, in the absence (black) or presence of 3 μM nicotine (red), and during wash-out (blue). Note the transition of a single AP with prominent ADP (under control conditions) into double spikes in the presence of nicotine. Scale bars for A–C and G–I are identical.

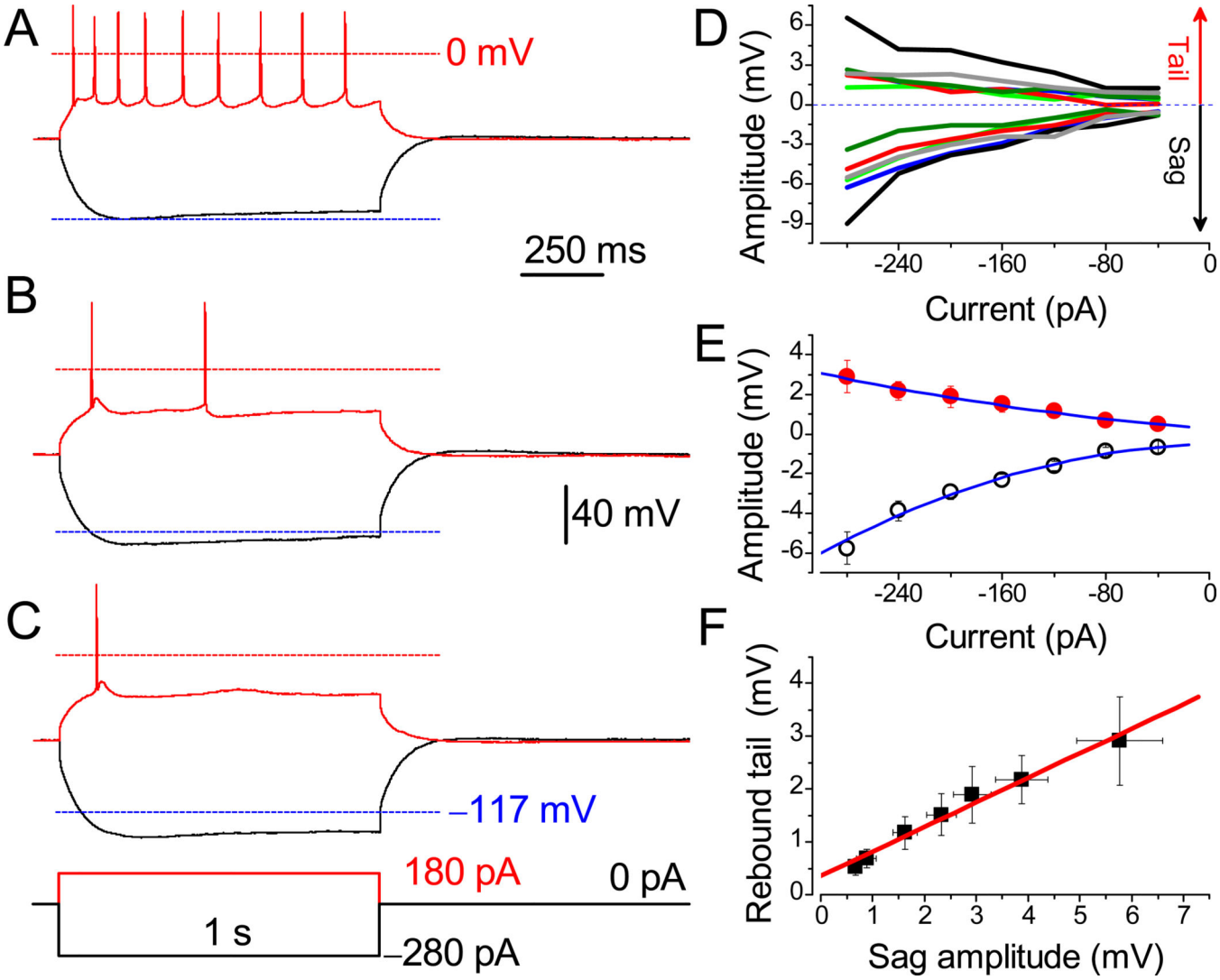

Fig. 4.

Suppression of evoked action potentials by nicotine in a subset of neurons. APs were evoked in LS neuron before (A) and after (B) treatment with 3 μM nicotine, and after 30 min wash-out (C). The APs were evoked from the RMP of −60.1 mV under identical conditions. Lower dashed lines are MP at −117 mV. Identical scale bars apply for A–C. (D) The sag and rebound tail potentials in different neurons are color-matched. (E) Mean amplitudes of rebound tail (●) and sag potentials (○, $n = 6$). Note that the amplitude of sag is two-fold greater than the tail potential. (F) The linear correlation between values of sag and tail potentials ($R = 0.99$).

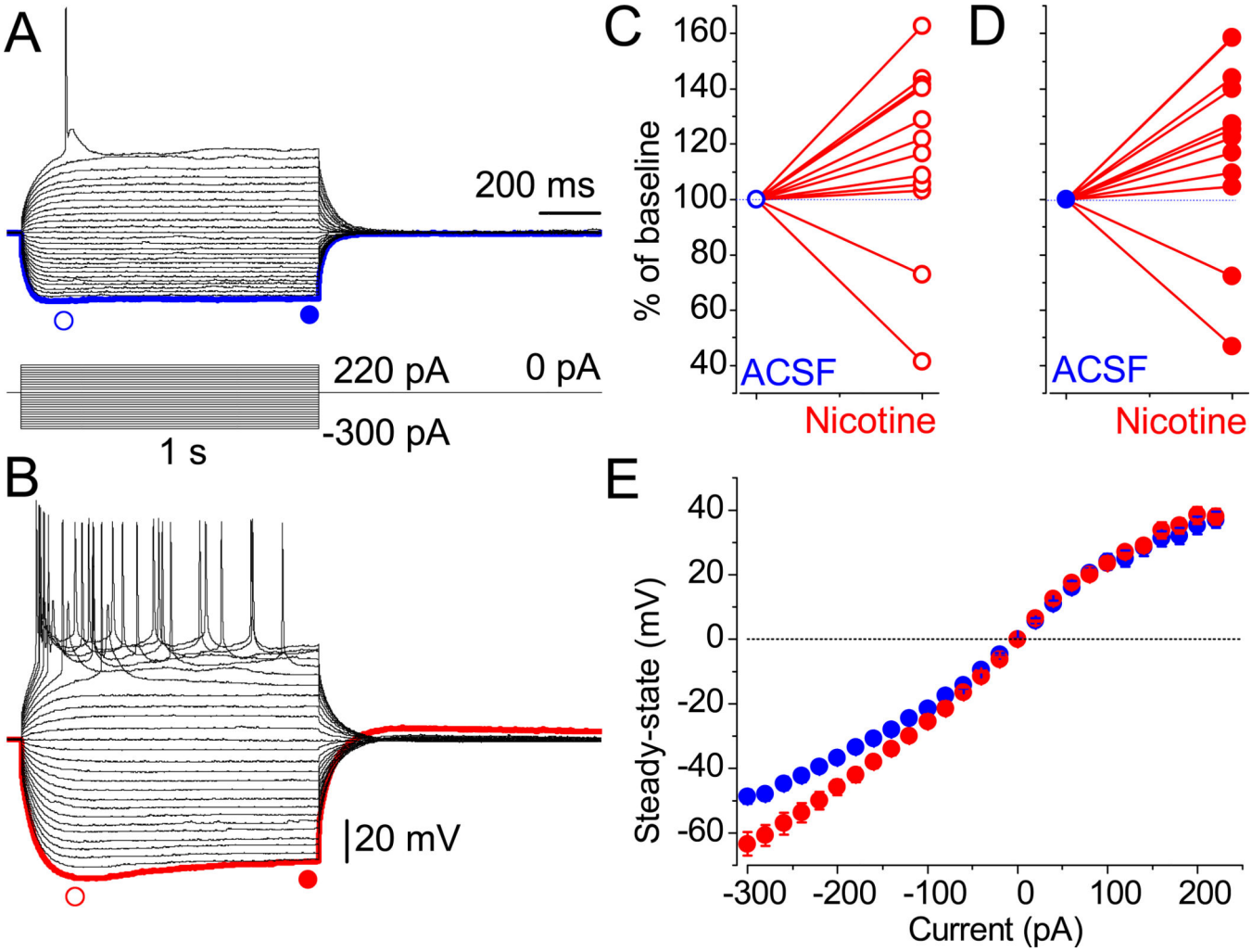

Fig. 5.

Nicotine-mediated sag. (A) The MP in neurons of the LS was recorded in response to hyperpolarizing currents under identical conditions, as in Figure 2. (B) Within 15 min of exposure to nicotine, sag and related rebound tail potentials appear. Scale bars for A and B are identical. The blue and red symbols indicate the points taken for statistical analyses. (C and D) The individually normalized peak and steady-state amplitude values for all tested neurons. (E) The mean amplitude values of the steady-state potentials were increased by nicotine only at more hyperpolarized MP (for example, at −200 pA: −45.8 ± 2.4 mV *vs.* −36.8 ± 1.7 mV, $n = 10$, $P = 0.001$). Error bars are very small under control conditions.

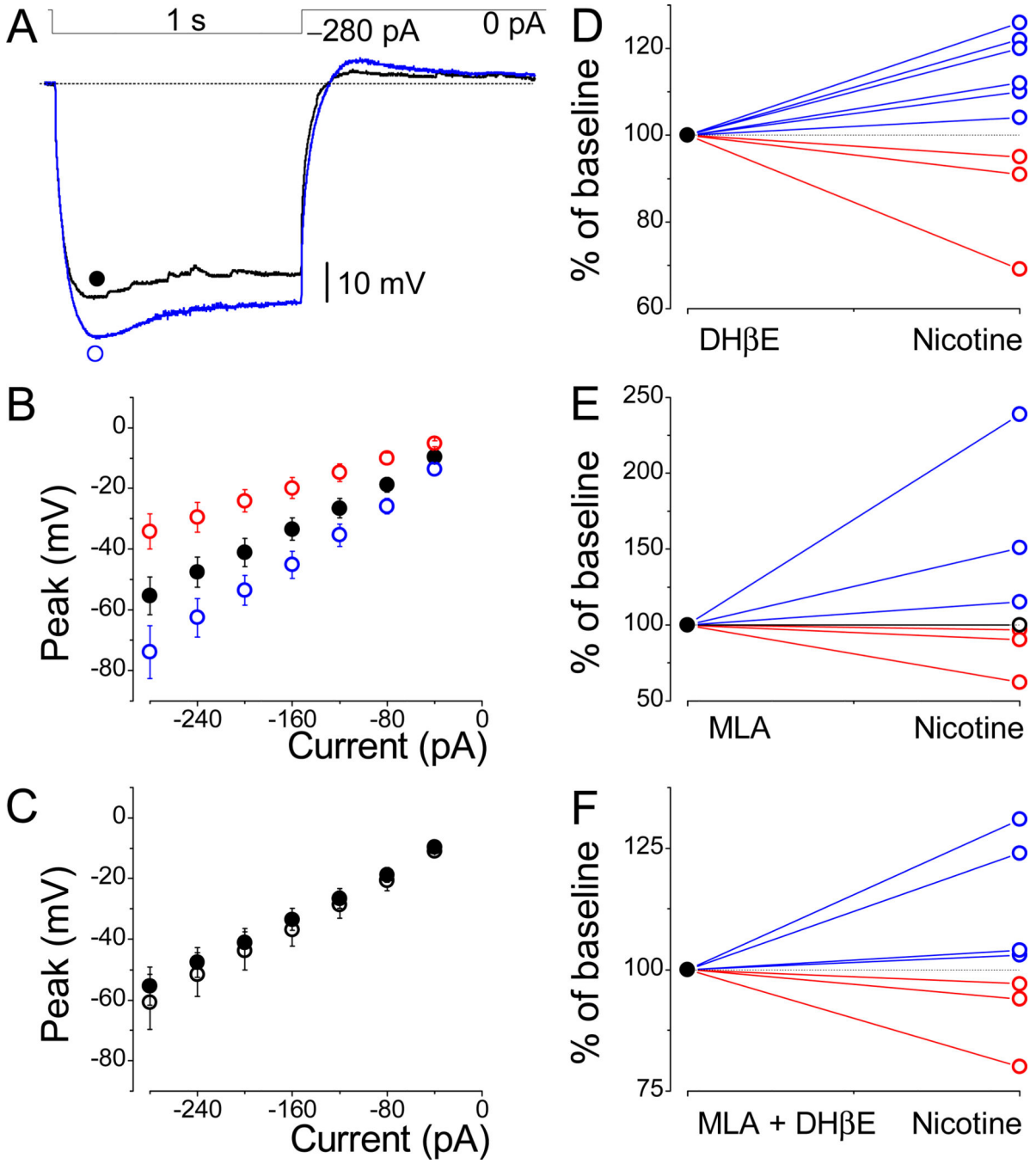

Fig. 6.

Effects of nicotine under nAChRs blockade. (A) Increase in sag and rebound tail potentials by nicotine despite the presence of antagonist, DHβE. Note the spontaneous postsynaptic potentials under control conditions. (B) Amplitude values obtained in the presence of 100 nM DHβE (●, $n = 9$). The presented data subdivide into two groups reflecting nicotine's dual effects: an increase (○, $n = 6$) and a decrease (○, $n = 3$) in peak amplitudes. (C) Under these conditions, values of pooled data for all neurons were not different in DHβE (●) and nicotine (○) sets of experiments ($n = 9$). (D–F) The individually normalized values for each

cell reveal the same tendency in the presence of either DHβE ($n = 9$), MLA (1 μM; $n = 7$), or both ($n = 7$). Note that only one cell (○) in E was not affected by nicotine in the presence of MLA. Scale bars are shown.

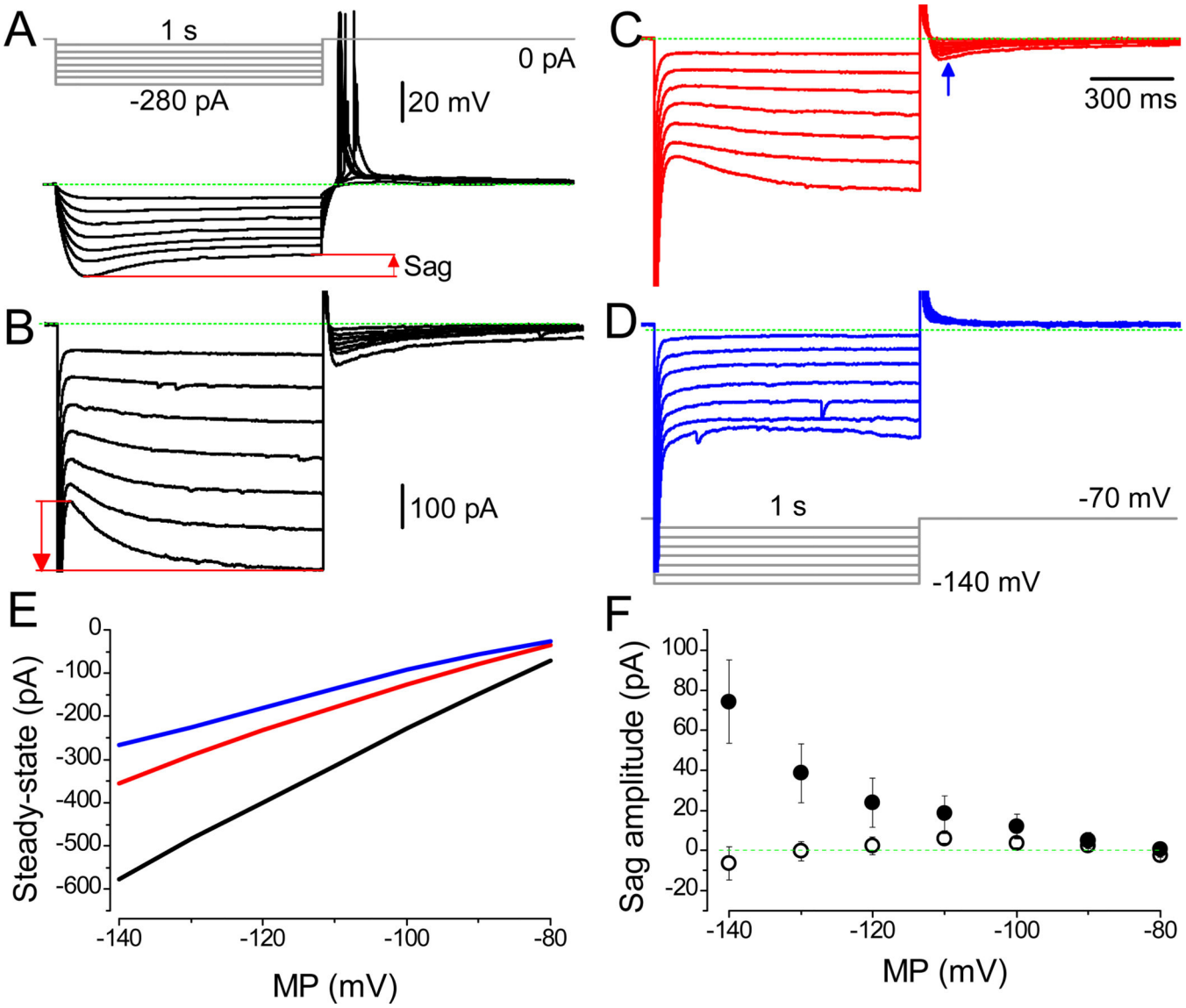

Fig. 7.

Selective inhibition of HCN channel mediated non-selective cationic currents. (A) The typical and comparable response of an LS neuron. Note RAPs upon termination of hyperpolarization; RMP: −63.9 mV. (B) Activation of I_h from the holding potential of −70 mV by the pulse protocol shown in D. The I_h, i.e. the counterpart of the sag potential, was observed readily at more hyperpolarized test potentials. (C and D) Dose-dependent decrease in amplitude by 1 and 10 μM ZD 7288, respectively. (E) The application of ZD 7288 affects the steady–state amplitudes. The I_h are shown under control conditions (black line) and in the presence of 1 μM (red) and 10 μM ZD 7288 (blue). (F) Consistently, the two groups confirming the absence (○, $n = 4$) and the presence (●, $n = 8$) of HCN-mediated currents are distinguished. The amplitude's scale bar for A is shown, while the time is reflected by the pulse protocol. Scale bars indicating current amplitude are identical for B–D.

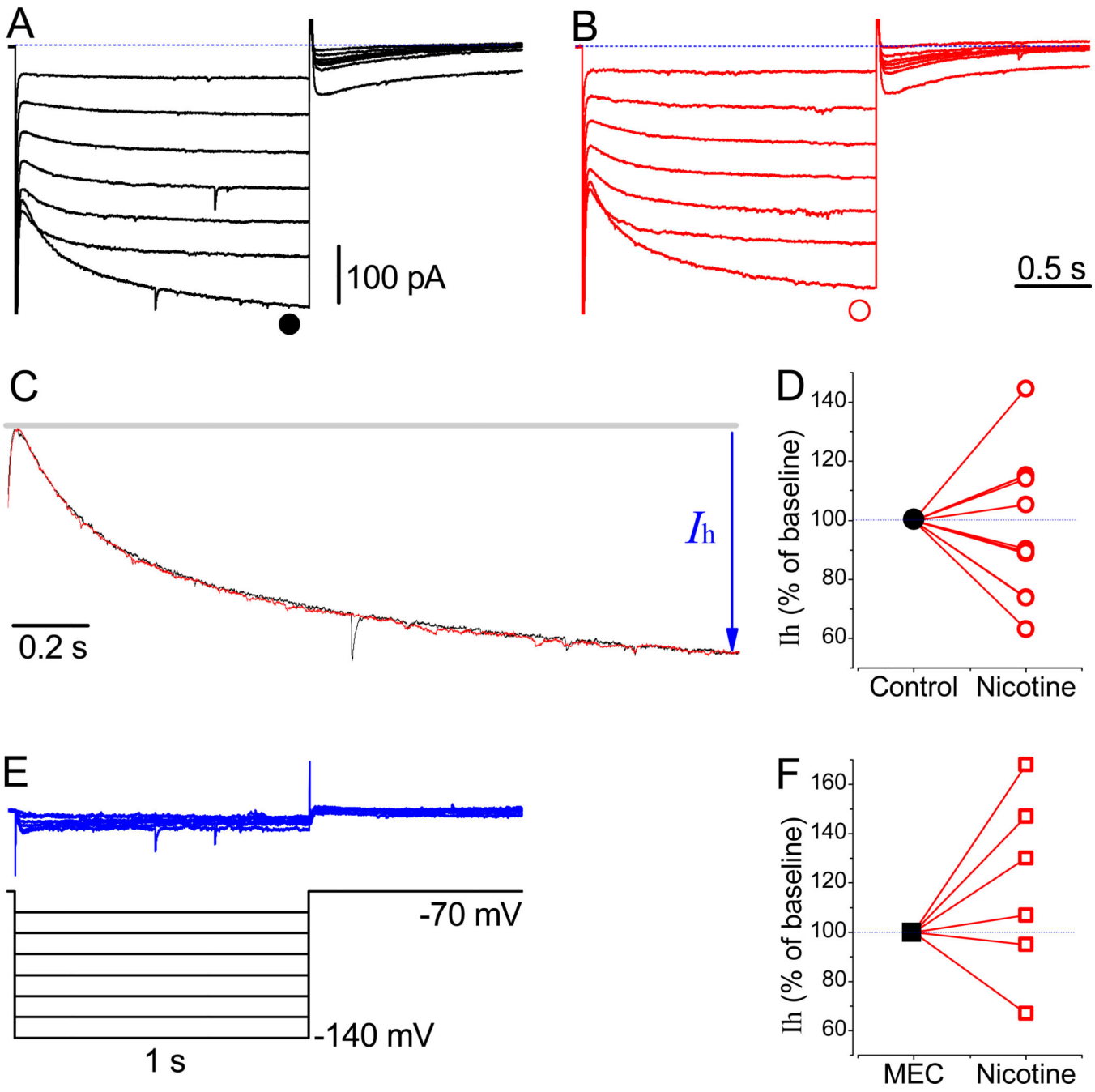

Fig. 8.

Effects of nicotine and MEC on I_h. (A) The I_h recorded at a holding potential of −70 mV using the protocol shown in E. (B) Traces are recorded 15 min after the application of 3 μM nicotine. (C) Normalized and superimposed traces revealing the similar activation kinetics of HCN channels in the absence of and the presence of nicotine at −140 mV, respectively. (D) Normalized I_h at −130 mV (●, $n = 11$). (E) The subtracted nicotine-sensitive currents. (F) Normalized I_h in the presence of a non-selective inhibitor of nAChRs, 10 μM MEC (■, $n = 6$). The time and amplitude scale bars are identical for A, B, and E.

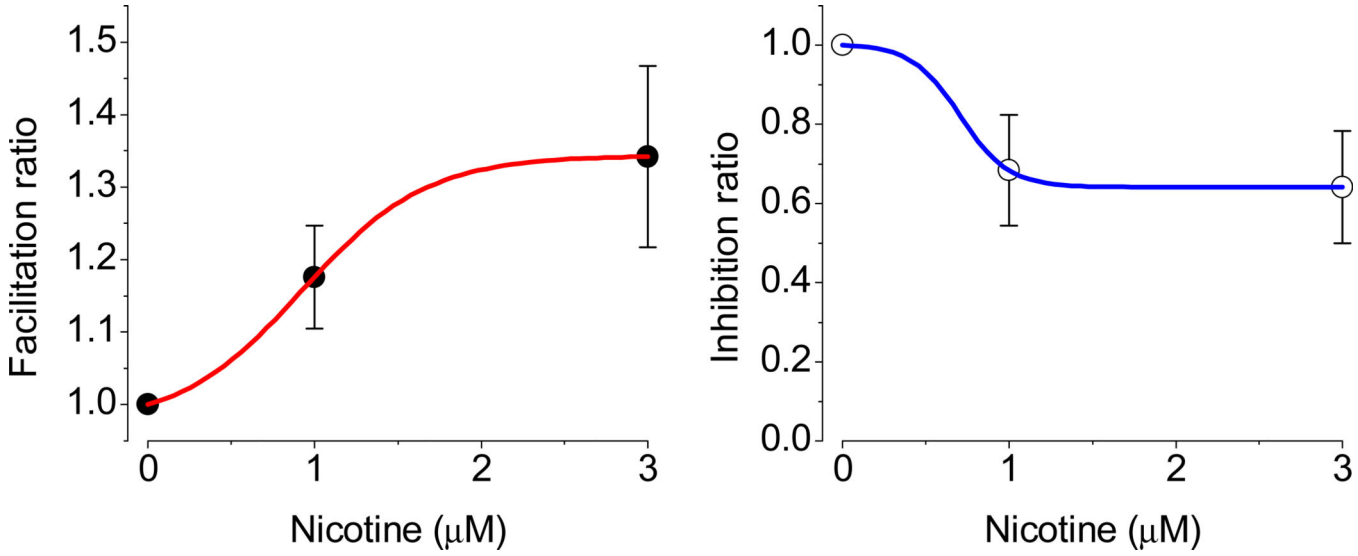

Fig. 9.

Cumulative dose response of nicotine in LS neurons. The facilitation and inhibition are shown for subgroups of neurons. Under identical experimental conditions, the facilitation saturated at 3 μM, while inhibition was already saturated at 1 μM ($n = 4$). The EC_{50} for facilitation was 0.92 μM ($n = 6$).